

# Improved SPRT Detection Using Localization with Application to Radiation Sources

Nageswara S. V. Rao, Charles W. Glover,  
Mallikarjun Shankar  
Oak Ridge National Laboratory  
Yong Yang  
University of Illinois at Urbana-Champaign

Jren-Chit Chin, David K. Y. Yau,  
Chris Y. T. Ma  
Purdue University  
Sartaj Sahni  
University of Florida

**Abstract** – We consider the problem of detecting a source with a scalar intensity inside a two-dimensional monitoring area using intensity sensor measurements in presence of a background process. The sensor measurements may be random due to the underlying nature of the source and background as well as due to sensor errors. The Sequential Probability Ratio Test (SPRT) can be used to infer detections from measurements at the individual sensors. When a network of sensors is available, these detection results may be combined using a fusion rule such as majority rule. We propose a detection method that first utilizes a robust localization method to estimate the source parameters and then employs an adaptive SPRT based on estimates to infer detection. Under Lipschitz conditions on the source and background parameters and minimum size of the packing number of state-space, we show that this method provides better performance compared to: (a) any SPRT-based single sensor detection with fixed threshold, and (b) majority and certain general fusers of SPRT-based single sensor detectors. We analyze the performance of this method for the case of detecting point radiation sources, and present simulation and testbed results.

**Keywords:** Sensor network, sequential probability ratio test, radiation source, detection and localization.

## 1 Introduction

We consider the detection of a source, which is characterized by its location and a scalar intensity, based on sensor measurements against a background process. The intensity of the source decays as one moves away from it and may reach levels comparable to that of the background. Sensor measurements contain random components due to measurement errors, or inherent randomness in the underlying source and background processes (such as radiation), or both. The a priori distribution as well as the intensity and location of the source are not known, but the functional form of sensor measurement distribution is known. We consider the

problem of detecting the presence of a source within the monitoring area by using measurements collected at the sensors. This formulation is motivated by the detection of point radiation sources, which has been studied extensively using single sensors [8, 1, 11]. With the advent of sensor network technologies, there has been a renewed interest in this problem [2, 9, 12, 18, 19], particularly motivated by ways to utilize measurements from networked sensors to achieve performance exceeding that of a single sensor.

For single sensors, the detection problem can be solved using a number of well-known methods [20, 21], and in particular the Sequential Probability Ratio Test (SPRT) has been shown to be quite effective for radiation sources [4, 6, 11]. The SPRT method relies on computing thresholds for the likelihood ratio test to infer the presence or absence of source or insufficiency of measurements to make such decision. When a network of sensors is available, SPRT can be used at the sensors, and the individual decisions can be fused [21]. In this approach, however, the fuser has access only to the Boolean detection information and not to the measurements nor to the inter-relationship between them. Such information, however, was found to be very useful in solving a different problem, namely, localization that estimates the location and intensity of source. But it is unclear if such improvements are possible in detection, even if only in certain cases. In this paper, we show that a suitably robust localization method, if available, can be utilized to improve detection to achieve performances superior to single sensor SPRT detectors as well as their majority and certain other fusers.

In the presence of a background process, the sensors always yield measurements with or without the source being present in the monitoring space. A localization method executed without asserting the detection first may lead to "ghost" sources. For example, in the case of detecting a point radiation source, the ghost source is within the vicinity of the centroid of sensor locations [15]. Primarily due to this reason, the localiza-

tion [3] is typically carried out post detection, that is only after asserting the presence of a source, for example using SPRT. However, it was recently shown that ghost sources can be eliminated using a suitable SPRT, somewhat surprisingly, more effectively than detecting the source itself. Such approach provided improved detection in simulations and testbed measurements, compared to SPRT based on a priori chosen threshold [11]. In this paper, we provide an analytical justification for this somewhat counter-intuitive approach that first estimates the source parameters and utilizes them in an adaptive SPRT to conclude detection. Our result is valid under the Lipschitz-separability condition on likelihood ratios and size of the packing number of the state-space of the source, and the availability of a suitably robust localization method. We show under these conditions, the detection and false alarm rates of a network of sensors can be made better using this approach compared to:

- (a) SPRT-based single sensor detection no matter how sophisticated a priori computed thresholds are;
- (b) majority fuser of SPRT-based detection of type (a) at the individual sensors; and
- (c) a generic class of fusers for detectors of type (a) that require detection by at least one sensor to assert their own detection.

The informal reasoning behind our result is as follows. A fixed-threshold SPRT detection method optimizes the detection performance within a certain neighborhood of state-space. Whereas the localization facilitates the adaptation of the threshold to each neighborhood of the state-space but only with a certain error probability. Then by trading-off the error probability of the localization method with the probability of "uncovered" regions of fixed-threshold SPRT, one can exceed the performance of the latter. We apply this approach for detecting point radiation sources, and derive detailed performance bounds. We also provide simulation and testbed results that illustrate our analytical results.

The rest of the paper is organized as follows. We show our main result that establishes the relative performance bounds on the detection and false alarm rates of the proposed method compared to fixed-threshold method in Section 2. We apply the general result to radiation detection problem in Section 3. We present our experimental results both using simulations and testbed measurements in Section 4

## 2 Detection Problem

We consider a two-dimensional monitoring area  $\mathcal{M} \subseteq \mathbb{R}^2$ , such as  $[0, D] \times [0, D]$ -grid, for detecting the presence of a source  $\mathcal{S}$  with unknown intensity  $A_S \in \mathcal{A}$ ,  $\mathcal{A} = (0, A]$ ,  $A < \infty$  located at an unknown location  $(x_S, y_S) \in \mathcal{M}$ . The source parameters  $(A_S, x_S, y_S) \in \mathbb{R}^+ \times \mathcal{M}$  constitute the *state-space*  $\mathcal{Z} = \mathcal{A} \times \mathcal{M}$ , and are distributed according to  $P_{(A_S, x_S, y_S)}$ . The source

appears inside  $\mathcal{M}$  with a priori probability

$$P_{\mathcal{M}} = \int_{A_S \in \mathcal{A}; (x_S, y_S) \in \mathcal{M}} dP_{(A_S, x_S, y_S)},$$

Both distributions  $P_{\mathcal{M}}$  and  $P_{(A_S, x_S, y_S)}$  are unknown. There is a background noise process characterized by the intensity parameter  $B_{(x, y)} \in \mathcal{B}$ ,  $\mathcal{B} = [0, B]$ ,  $B < \infty$  that depends on the location  $(x, y) \in \mathbb{R}^2$ , and thus background noise process is parametrized by  $P_{(B_{(x, y)}, x, y)}$ .

Let  $M_i = (x_i, y_i) \in \mathbb{R}^2$ ,  $i = 1, 2, \dots, N$ , be the locations of sensors deployed to monitor the area  $\mathcal{M}$ ; the sensors may not necessarily be located inside  $\mathcal{M}$ . For any point  $P = (x, y) \in \mathbb{R}^2$ , we have the distance  $d(P, M_i) = \sqrt{(x - x_i)^2 + (y - y_i)^2}$ , for  $1 \leq i \leq N$ . For two points in state-space  $z_1 = (a_1, x_1, y_1)$ ,  $z_2 = (a_2, x_2, y_2) \in \mathcal{Z}$ , we define  $d(z_1, z_2) = \sqrt{(a_1 - a_2)^2 + (x_1 - x_2)^2 + (y_1 - y_2)^2}$ . The sensor measurements are characterized as follows:

- (a) **Background Measurements:** When there is no source present, the "background" measurements of  $M_i$  are distributed according to  $P_{B_i}$ ,  $B_i = B_{(x_i, y_i)}$ .
- (b) **Source Measurements:** When the source is present in  $\mathcal{M}$ , the intensity at sensor location  $(x_i, y_i)$  is  $A_i$  which is a function of  $A_S$  and  $d(S, M_i) = d((x_S, y_S), M_i)$ . We represent this dependence explicitly as a function  $A_i = F_S(A_S, x_S, y_S, x_i, y_i)$ . The measurements of  $A_i$  collected at  $M_i$  are distributed according to  $P_{A_i + B_i}$ .

It is assumed that the underlying measurement distributions  $P_{B_i}$  and  $P_{A_i + B_i}$  are known; for the example for detecting point radiation sources, these distributions are approximated by Poisson process with parameters  $B_i$  and  $A_i + B_i$ , respectively [8, 1, 11]. Let  $m_{i,1}, m_{i,2}, \dots, m_{i,n}$  be the sequence of measurements collected by sensor  $M_i$  over an observation time window  $W$ , such that  $m_{i,t}$ ,  $i = 1, 2, \dots, N$ , are collected at the same time  $t$  at all sensors.

We consider the *Detection Problem* that deals with inferring the presence of a source inside  $\mathcal{M}$  based on measurements collected at  $M_1, M_2, \dots, M_N$ . We characterize the solution of the detection problem by the (a) *false alarm probability*  $P_{0,1}$ , corresponding to the probability of declaring the presence of a source when none exists, and (b) *missed detection probability*  $P_{1,0}$ , corresponding to the probability of declaring the presence of only the background radiation when a source is present in the monitoring area. The detection probability is given by  $P_{1,1} = 1 - P_{1,0}$ .

The main challenge of the detection arises due to the underlying randomness of measurements. The source intensity levels at sensor locations may only be slightly above background levels for low-level sources when sensors are located far away. Then the randomness in

sensor measurements makes it difficult to distinguish source signal amidst background noise. For example, the high variance of the measurements due to radiation sources makes this task particularly challenging.

## 2.1 SPRT Detection

Consider the measurements  $m_{i,1}, m_{i,2}, \dots, m_{i,n}$  collected by sensor  $M_i$  within a given time window and the background radiation level  $B_i = B_{(x_i, y_i)}$  at this sensor location. Let  $H_C$ , for  $C \in \{A_i + B_i, B_i\}$ , denote the hypothesis that the measurements correspond to intensity level  $C$  at the sensor  $M_i$ . Now consider the likelihood function  $L(m_{i,1}, m_{i,2}, \dots, m_{i,n} | H_C)$  which represents the probability that the measurements were produced by the source if  $C = A_i + B_i$  and just the background if  $C = B_i$ . The ratio of these likelihood functions can be utilized to decide between these hypotheses. We now consider the following SPRT based on sensor measurements at  $M_i$

$$\mathcal{L}_{A_i, B_i, n} = \frac{L(m_{i,1}, m_{i,2}, \dots, m_{i,n} | H_{A_i+B_i})}{L(m_{i,1}, m_{i,2}, \dots, m_{i,n} | H_{B_i})}$$

which can be used for detecting the source with false positive and missed detection probability parameters  $P_{0,1}$  and  $P_{1,0}$  respectively as follows [7]:

- (i) If  $\mathcal{L}_{A_i, B_i, n} < \frac{P_{0,1}}{1-P_{1,0}}$ , then declare the background, namely  $H_{B_i}$ ;
- (ii) Else if  $\mathcal{L}_{A_i, B_i, n} > \frac{1-P_{0,1}}{P_{1,0}}$ , then declare that a source is present, that is  $H_{A_i+B_i}$ ;
- (iii) Otherwise, declare that the measurements are not sufficient to make a decision and continue collecting additional measurements.

The following properties of the SPRT [7] make this test suitable for the present detection problem: (a) The expected false alarm and miss detection rates of SPRT are given by  $P_{1,0}$  and  $P_{0,1}$ , respectively. (b) Among all tests to decide between  $H_{A_i+B_i}$  and  $H_{B_i}$  with the given  $P_{1,0}$  and  $P_{0,1}$ , SPRT minimizes  $E[n|H_{B_i}]$  and  $E[n|H_{A_i+B_i}]$  (see Theorem 2.4, [22], for example).

This test can be compactly expressed as

$$\frac{P_{0,1}}{1-P_{1,0}} \leq \mathcal{L}_{A_i, B_i; n} \leq \frac{1-P_{0,1}}{P_{1,0}}$$

Typically,  $\mathcal{L}_{A_i, B_i; n}$  cannot be directly applied for our detection problem since it depends on  $A_i$  which in turn depends on source location and intensity both of which are unknown. By utilizing the domain knowledge, this test is often expressed in terms of measurements, and we consider such a generic case. We define likelihood ratio test to be *separable* if it can be expressed as

$$\begin{aligned} F_L(P_{0,1}, P_{1,0}, A_i, B_i) &< \sum_{j=1}^n m_{i,j} \\ &< F_U(P_{0,1}, P_{1,0}, A_i, B_i), \end{aligned}$$

for suitable lower and upper threshold function  $F_L(\cdot)$  and  $F_U(\cdot)$ , respectively. However, the test in this form is also not exactly implementable since the upper and lower threshold values now depend on the unknown source parameters. In practice suitable scalar values  $\tau_L$  and  $\tau_H$  are chosen for the upper and lower thresholds respectively, based on domain-specific considerations, Bayesian inference or other method (in addition to choosing appropriate values for  $P_{1,0}$  and  $P_{0,1}$ ). In particular, such approach has been quite extensively used in the detection of radiation sources [11]. We denote the SPRT with such selected threshold by  $\mathcal{L}_{\tau_L, \tau_H}$ , which will be called *fixed-threshold* SPRT.

We define a separable SPRT to be *Lipschitz-separable* if the threshold functions are Lipschitz in the following sense: for any  $P_{0,1}, P_{1,0}, B_i$ , there exists scalars  $K_L$  and  $K_U$  such that

$$\begin{aligned} |F_L(\cdot, A_i, \cdot) - F_L(\cdot, A_i + \gamma, \cdot)| &\leq K_L \gamma, \quad \text{and} \\ |F_U(\cdot, A_i, \cdot) - F_U(\cdot, A_i + \gamma, \cdot)| &\leq K_U \gamma. \end{aligned}$$

The Lipschitz parameters  $K_L$  and  $K_U$  denote the sensitivity of the threshold functions to intensity value at sensor  $M_i$ , which in turn depends both on source location and intensity through the function  $A_i = F_S(A_S, x_S, y_S, x_i, y_i)$ .

We define the source to be *Lipschitz* if its intensity at sensor location  $A_i = F_S(A_S, x_S, y_S, x_i, y_i)$  satisfies the following condition: there exists scalars  $K_A$ ,  $K_x$ , and  $K_y$  such that

- (a) for any  $x_S, y_S, x_i$  and  $y_i$ , we have

$$|F_S(A_S, \cdot) - F_S(A_S + \gamma, \cdot)| \leq K_A \gamma$$

- (b) for any  $A_S, x_i, y_i$ , we have

$$\begin{aligned} |F_S(\cdot, x_S, \cdot) - F_S(\cdot, x_S + \gamma, \cdot)| &\leq K_x \gamma, \quad \text{and} \\ |F_S(\cdot, y_S, \cdot) - F_S(\cdot, y_S + \gamma, \cdot)| &\leq K_y \gamma. \end{aligned}$$

Thus for a Lipschitz source with Lipschitz-separable SPRT the lower threshold function  $F_L(\cdot)$  is Lipschitz with respect to the source parameters  $A_S, x_S$  and  $y_S$  with constants  $K_L K_A, K_L K_x$  and  $K_L k_y$ , respectively; similarly the upper threshold function  $F_U(\cdot)$  is Lipschitz with constants  $K_U K_A, K_U K_x$  and  $K_U k_y$ , respectively. We will show in next section that these Lipschitz conditions are satisfied in the case of point radiation sources.

## 2.2 Detection Using Localization

The *localization problem*<sup>1</sup> is concerned with estimating the location and strength of the source using measurements  $m_{i,j}, i = 1, 2, \dots, N, j = 1, 2, \dots, T$ . The

<sup>1</sup>Localization is not addressed in this paper as a problem to be solved; rather, localization is proposed as a means to solving the detection problem. In some formulations localization refers to just estimating the source location, and the estimation of the source strength is referred to as the identification problem. Here we refer to localization in the generic parameter space  $\{(A_S, x_S, y_S) \in A \times \mathcal{M}\}$ .

estimates of  $A_S$  and  $(x_S, y_S)$  are denoted by  $\hat{A}_S$  and  $(\hat{x}_S, \hat{y}_S)$ , respectively.

To solve the detection problem using localization, we first estimate the source parameters and use them in the SPRT as follows:

$$F_L(P_{0,1}, P_{1,0}, \hat{A}_i, B_i) < \sum_{j=1}^n m_{i,j} < F_U(P_{0,1}, P_{1,0}, \hat{A}_i, B_i)$$

such that  $\hat{A}_i = F(\hat{A}_S, \hat{x}_S, \hat{y}_S, x_i, y_i)$ . We denote the SPRT as  $\mathcal{L}_{\hat{S}}$ , and refer to as the *localization-based SPRT*. When a localization algorithm is executed using “background” measurements, the estimated parameters correspond to ghost sources. We show in the next section that the absence of ghost source and hence presence of real source (namely detection) can be asserted more effectively than  $\mathcal{L}_{\tau_L, \tau_H}$  executed on direct measurements, thereby improving the detection rate. Also, the presence of ghost source and hence the absence of real source can be more effectively asserted compared no-detection by  $\mathcal{L}_{\tau_L, \tau_H}$ , thereby improving the false alarm rate of the latter.

### 2.3 Comparison of $\mathcal{L}_{\tau_L, \tau_H}$ and $\mathcal{L}_{\hat{S}}$

In this section, we provide analytical justification and quantification of performance improvements of  $\mathcal{L}_{\hat{S}}$ . We define a localization method to be  $\delta$ -robust if the following condition can be ensured: there exists  $\delta(\epsilon, n, N)$ , which is a non-increasing function of number of measurements  $n$  and number of sensors  $N$  and non-decreasing function of precision  $\epsilon$  such that

$$P \left\{ (\hat{x}_S, \hat{y}_S, \hat{A}_S) \in \mathfrak{R}_{S, \epsilon} \right\} > \delta(\epsilon, n, N)$$

where  $\mathfrak{R}_{S, \epsilon} = \{z \in \mathfrak{R}^3 | d(z, z_S) \leq \epsilon; z_S = (A_S, x_S, y_S)\}$  called  $\epsilon$ -precision region. This condition ensures that the estimate is within  $\epsilon$  of source parameter  $z_S$  with probability  $\delta$ , which improves as more measurements are collected and more sensors are deployed. Also, smaller values of  $\epsilon$  are achieved with lower probability. This condition is a reasonable requirement and is satisfied by algorithms used for localizing point radiation sources [16, 14].

For a given SPRT  $\mathcal{L}$ , we denote the detection and false alarm probabilities by  $\mathcal{E}_D(\mathcal{L})$  and  $\mathcal{E}_F(\mathcal{L})$ , respectively. A *spherical cell* with center  $z_k \in \mathfrak{R}^3$  and radius  $\rho$  is defined as  $\mathcal{C}(z_k) = \{z | d(z, z_k) < \rho\}$ . A  $\rho$ -packing of state-space  $\mathcal{Z} = \mathcal{A} \times \mathcal{M}$  corresponds to disjoint spherical cells with *cell centers* at  $z_k, k = 1, 2, \dots, K$  of radius  $\rho$  all contained inside state-space  $\mathcal{Z}$ . We define such a packing to be *translation invariant* if all cells are still inside  $\mathcal{Z}$  when centers are translated as  $z + z_k$ , for all  $z \in \mathcal{Z}$ . Let *state packing number*  $\mathcal{N}(\mathcal{Z}, \rho)$  denote the maximum size of translation invariant  $\rho$ -packing of the state-space  $\mathcal{Z}$ .

We define two sets that represent all possible sources that correspond to the thresholds of  $\mathcal{L}_{\tau_L, \tau_H}$  as follows:

$$\mathcal{S}_{\tau_L} = \{z \in \mathcal{Z} \mid \tau_L = F_L(P_{0,1}, P_{1,0}, A_i, B_i); A_i = F_S(A_S, x_S, y_S, x_i, y_i)\} \text{ and}$$

$$\mathcal{S}_{\tau_H} = \{z \in \mathcal{Z} \mid \tau_H = F_H(P_{0,1}, P_{1,0}, A_i, B_i); A_i = F_S(A_S, x_S, y_S, x_i, y_i)\}.$$

The following theorem characterizes the relative performance of the threshold-based SPRT  $\mathcal{L}_{\tau_L, \tau_H}$  and localization-based SPRT  $\mathcal{L}_{\hat{S}}$ .

**Theorem 2.1** *Consider the detection of a Lipschitz source with Lipschitz-separable SPRT. Then for SPRT  $\mathcal{L}_{\hat{S}}$  based on  $\delta$ -robust localization method and any threshold-based SPRT  $\mathcal{L}_{\tau_L, \tau_H}$ , for sufficiently large  $n$  and  $N$ :*

(i) *detection rates satisfy*

$$\mathcal{E}_D(\mathcal{L}_{\hat{S}}) > [\mathcal{E}_D(\mathcal{L}_{\tau_L, \tau_H}) + (\mathcal{N}(\mathcal{Z}, \kappa \rho_D) - 1)] \delta(\rho_D, n, N);$$

(ii) *false alarm rates satisfy*

$$\mathcal{E}_F(\mathcal{L}_{\hat{S}}) < [\mathcal{E}_F(\mathcal{L}_{\tau_L, \tau_H}) - (\mathcal{N}(\mathcal{Z}, \kappa \rho_F) - 1)] \delta(\rho_F, n, N)$$

where  $\kappa = K_U \max\{K_A, K_x, K_y\}$ ,  $\rho_D = \max_{z_1, z_2 \in \mathcal{S}_{\tau_H}} d(z_1, z_2)$  and  $\rho_F = \max_{z_1, z_2 \in \mathcal{S}_{\tau_L}} d(z_1, z_2)$ .

**Proof:** The outline of the proof is similar in both cases: we compute a spherical cell for  $\mathcal{L}_{\tau_L, \tau_H}$  in which it does not make an error and utilize the Lipschitz property to compute the underlying  $\rho$  value,  $\rho_D$  for detection rate and  $\rho_F$  for false alarm rate. Then we utilize this as  $\epsilon$  value for the  $\mathcal{L}_{\hat{S}}$  and exploit the monotonicity of  $\delta$  in  $n$  and  $N$  to ensure that  $\hat{S}$  is within  $\rho$ -precision region. Then we compute the  $\rho$ -packing of the state-space and identify the cell corresponding to  $\mathcal{L}_{\tau_L, \tau_H}$ , and in all other cells  $\mathcal{L}_{\hat{S}}$  does not make an error with probability  $\delta$  and hence offers better performance than the former. We now provide the details of the bound on the detection rate in Part (i), which assumes that the source is present. Let  $\mathcal{S}_{\tau_L}$  and  $\mathcal{S}_{\tau_H}$  denote the centroids of  $\mathcal{S}_{\tau_L}$  and  $\mathcal{S}_{\tau_H}$ , respectively, and let  $\mathcal{C}_{\tau_L}$  and  $\mathcal{C}_{\tau_H}$  denote the spherical cells of radius  $\rho_D$  centered at them, respectively. Now consider a  $\kappa \rho_D$ -packing of the state-space (translated if needed) such that one of its spherical cells  $\mathcal{C}_{\tau_H}$  aligns exactly with  $\mathcal{S}_{\tau_H}$ . For fixed  $\tau_L$  and  $\tau_H$ ,  $\mathcal{L}_{\tau_L, \tau_H}$  does not make an error if the source lies inside  $\mathcal{C}_{\tau_H}$ ; but it will make an error everywhere else, in particular on all the other spherical cells of  $\kappa \rho_D$ -packing of the state-space. There are at least  $\mathcal{N}(\mathcal{Z}, \kappa \rho_D)$  spherical cells inside state-space, and only one corresponds

to  $\mathcal{S}_{\tau_H}$  over which it does not make an error. On the other hand,  $\mathcal{L}_{\hat{S}}$  does not make an error on any of the spherical cell but with probability  $\delta$ . Thus the detection probability of  $\mathcal{L}_{\hat{S}}$  corresponding to these spheres is at least  $[(\mathcal{N}(\mathcal{Z}, \rho_D) - 1)] \delta(\rho_D, n, N)$ . For the sphere  $\mathcal{C}_\tau$  however detection by  $\mathcal{L}_{\tau_L, \tau_H}$  is with probability 1 and that by  $\mathcal{L}_{\hat{S}}$  is with  $\delta$ , which leads to the inequality in Part (i).  $\square$

This theorem shows that performance, in terms of both  $\mathcal{E}_D$  and  $\mathcal{E}_F$ , of  $\mathcal{L}_{\hat{S}}$  is better than  $\mathcal{L}_{\tau_L, \tau_H}$  by the factor proportional to the packing number  $\mathcal{N}(\mathcal{Z}, \kappa\rho_D)$  and  $\delta(\cdot)$ . The performance bounds are valid no matter how thresholds are chosen for  $\mathcal{L}_{\tau_L, \tau_H}$ , for example, using domain-specific knowledge as in radiation source detection, Bayesian inference, and Dempster-Shafer theory. Informally speaking, “larger” monitoring space will have larger packing number, and hence the  $\mathcal{L}_{\hat{S}}$  will lead to more effective detection. In particular, performance of  $\mathcal{L}_{\hat{S}}$  will be increasingly better as one considers larger state-spaces, more sensors and more measurements. The limiting case  $\mathcal{N}(\mathcal{Z}, \kappa\rho_D) = 1$  corresponds to entire monitoring space being packed by a single sphere; in this case any source estimate within this sphere is just as accurate as  $\mathcal{L}_{\hat{S}}$ .

This approach of Theorem 2.1 can be used to derive more general results. The source intensity could be a finite dimensional vector and the source location can be specified in higher dimensional space, for example to include 3-D location and velocity. In this theorem, single scalar parameters  $\rho_D$  and  $\rho_F$  characterize the precision in  $A_S$ -space as well as  $x_S$ - and  $y_S$ -spaces. In general, different state-space parameters may be specified at different scales, and in such case it is direct to adapt the result by appropriately defining the spherical cells of the state-space packing. One can utilize different distance type such as  $d_{\max}(z_S, z) = \max\{|A_S - A|, |x_S - x|, |y_S - y|\}$  in the above result by noting that  $d_{\max}(z_S, z) \leq d(z_S, z) \leq 3d_{\max}(z_S, z)$  and hence  $\mathcal{N}(\mathcal{Z}, 3d_{\max}) \leq \mathcal{N}(\mathcal{Z}, d) \leq \mathcal{N}(\mathcal{Z}, d_{\max})$ .

## 2.4 Comparison of $\mathcal{L}_{\hat{S}}$ and Fusers

When SPRT is executed at each of  $N$  sensors with possibly different threshold limits, the individual detection results may be combined at the fusion center using methods such as majority fuser or Bayesian fuser. Consider that the state-space is large enough that  $\mathcal{N}(\mathcal{Z}, \kappa\rho_D) \geq N$ . For the majority fuser, denoted by  $\mathcal{L}_M$ , a direct application of the proof method in Theorem 1 shows that it makes a correct detection on at most  $N$  spherical cells. But  $\mathcal{L}_{\hat{S}}$  will make correct decision on all spherical cells, and thus we have  $\mathcal{E}_D(\mathcal{L}_{\hat{S}}) > [\mathcal{E}_D(\mathcal{L}_M) + (\mathcal{N}(\mathcal{Z}, \kappa\rho_D) - N)] \delta(\rho_D, n, N)$ , for  $\mathcal{N}(\mathcal{Z}, \rho_D) \geq N$ .

We now show that the same performance bound is valid for a more general class of fusers. We consider a broad class of fusers  $\mathcal{F}_1$  such that fuser  $F_1 \in \mathcal{F}_1$  declares a detection only if at least one sensor declares detection,

i.e., it does not declare a detection if none of the sensors declare a detection. This fuser class excludes the fusers that exploit the cases when the individual SPRTs consistently under-perform (such as less than 50% accuracy) by simply flipping their outputs. While this class does not include all possible fusers, it includes a wide class where the fuser is effective when some of the individual SPRTs are effective. Any such fuser  $F_1$  makes a correct detection on at most  $N$  sphere cells, but will make a error on other cells that constitute the packing number, hence the above bound is satisfied for this general class of fusers. Compared to  $\mathcal{L}_{\tau_L, \tau_H}$ , the performance improvements of  $\mathcal{L}_{\hat{S}}$  over  $\mathcal{L}_M$  or  $\mathcal{L}_{F_1}$  require a larger packing number. Intuitively, such stronger requirement is expected since fusers in general perform better than single sensors.

## 3 Radiation Source Detection

We consider the identification of a point radiation source  $S$  of unknown strength  $A_S$  expressed as Counts Per Minute (CPM) called the *source rate*, and located at an unknown location  $(x_S, y_S)$ . The source gives rise to a radiation intensity of  $A_i = A_S/d_i^2$  at sensor location  $(x_i, y_i)$ , where  $d_i = d((x_S, y_S), M_i)$ . This radiation source is Lipschitz with constants  $K_A$ ,  $K_x$  and  $K_y$  estimated by using the partial derivatives of  $A_i = F_S(A_S, x_S, y_S, x_i, y_i)$  as follow:

$$K_A = \frac{\partial F_S}{\partial A_S} = 1/d_i^2$$

$$K_x = \frac{\partial F_S}{\partial x_S} = \frac{A_S |x_S - x_i|}{d_i^3}$$

$$K_y = \frac{\partial F_S}{\partial y_S} = \frac{A_S |y_S - y_i|}{d_i^3}.$$

The radiation count  $m_{i,j}$  observed at  $M_i$  at time  $j$  is a Poisson random variable with parameter  $\lambda = B_i = B(x_i, y_i)$  when there is no source present, and with  $\lambda = A_i + B_i$ , when source is present [8, 10]. In either case, the measurements are statistically independent across time, and exhibit significant variations shown in Figure 1. The likelihood function in this case is:

$$L(m_{i,1}, m_{i,2}, \dots, m_{i,n} | H_C) = \prod_{j=1}^{n_i} \frac{C^{m_{i,j}} e^{-C}}{m_{i,j}!}$$

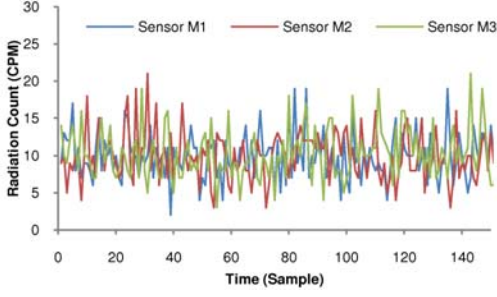
where  $C \in \{B_i, A_i + B_i\}$ .

The SPRT for detecting a radiation source can be expressed in terms of the sum of measurements as:

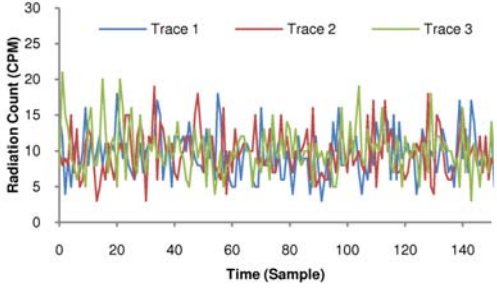
$$\frac{\ln \left[ \frac{F_{0,1}}{1 - F_{1,0}} \right] + n A_i}{\ln \left[ \frac{A_i + B_i}{B_i} \right]} \leq \sum_{j=1}^n m_{i,j} \leq \frac{\ln \left[ \frac{1 - F_{0,1}}{F_{1,0}} \right] + n A_i}{\ln \left[ \frac{A_i + B_i}{B_i} \right]}$$

which shows that it is separable. In addition, this SPRT is Lipschitz-separable with constants  $K_L$  and  $K_U$  given by:

$$K_L = \frac{\partial F_L}{\partial A_i} < \frac{n}{\ln \left( \frac{A_i + B_i}{B_i} \right)}; \quad K_U = \frac{\partial F_U}{\partial A_i} < \frac{n}{\ln \left( \frac{A_i + B_i}{B_i} \right)}.$$



(a) Measurements from RFTrax radiation sensors.



(b) Simulated Poisson variables with  $\lambda = 10$ .

Figure 1: Background radiation shows high variance.

Thus the Lipschitz constants of  $F_U(\cdot)$  with respect to  $A_S$ ,  $x_S$  and  $y_S$  are given as follows, respectively:

$$K_U K_A = \ln \left( \frac{A_i + B_i}{B_i} \right) / d_i$$

$$K_U K_x = \ln \left( \frac{A_i + B_i}{B_i} \right) \frac{A_S |x_S - x_i|}{d_i^3}$$

$$K_L K_y = \ln \left( \frac{A_i + B_i}{B_i} \right) \frac{A_S |y_S - y_i|}{d_i^3}.$$

Lipschitz constants of  $F_L(\cdot)$  can be similarly computed.

We now compute a lower bound on  $\mathcal{N}(\mathcal{Z}, \rho)$ ,  $\rho = \kappa \rho_D$ , for the monitoring region  $[A_{\min}, A] \times [0, D] \times [0, D]$ . A minimum number of 1-dimensional spherical cells of radius  $\rho$  that can be packed along  $A$ -axis is  $n_A = \frac{A}{\alpha} \left( \frac{d_i}{\rho} \right)$ , where  $\alpha = \ln \left( \frac{A_i + B_i}{B_i} \right)$ . Similarly, such number along  $x$  and  $y$  axes is given by  $n_x = n_y = \frac{D}{\alpha} \left( \frac{d_i}{A_S} \right) \left( \frac{d_i}{\rho} \right)$ . Thus, we have

$$\mathcal{N}(\mathcal{Z}, \rho) \geq \min \frac{d_i}{\rho D} \left\{ A/\alpha, D/\alpha \left( \frac{d_i}{A_S} \right) \right\}.$$

This bound increases as larger monitoring spaces (larger  $D$ ) are considered, and larger separation between the source and sensors (larger  $d_i$ ) is considered. Under these conditions, the relative performance of  $\mathcal{L}_{\hat{S}}$  gets increasingly better compared any fixed threshold method  $\mathcal{L}_{\tau_i, \tau_H}$ .

There are several localization algorithms proposed for radiation sources, including adapting Gaussian model in [5], geometric method called the Difference Time Of Arrival (DTOA) method [17, 15], mean of estimates method [16], and iterative pruning method [3]. The

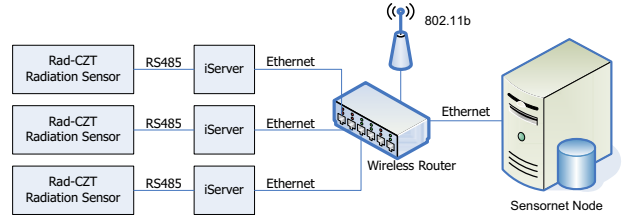


Figure 2: Equipment setup in the radiation test-bed.

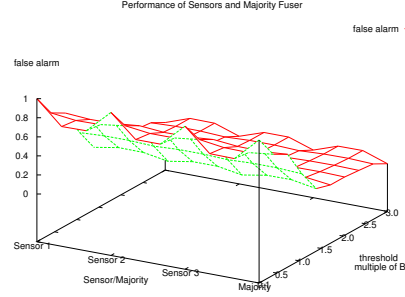


Figure 3: False alarm rate for different thresholds.

DTOA method to estimate  $(\hat{x}_u, \hat{y}_u)$  is shown to be  $\delta$ -robust in  $(x, y)$ -space [17, 16], and we will present experimental results using this and iterative pruning method in the next section.

## 4 Experimental Results

### 4.1 Simulation Results

We simulated radiation sources to be located uniformly inside  $[0, 1000] \times [0, 1000]$  spatial grid with  $A$  chosen from  $[1, 10^{12}]$  with  $B_{(x,y)} = 10$ . Sensors  $M_1$  and  $M_2$  are located at  $(0, 0)$  and  $(0, 1000)$  on the grid and  $M_3$  is such that  $y_3 = 1000$  and  $x_3$  is uniformly chosen from  $[0, 1000]$ . The simulation programs are implemented in C using random number generators from Numerical Recipes [13] and executed on a Redhat Linux workstation with a 2.8 GHz Intel processor.

We first present two illustrative cases, with and without the source present. We first consider the case of background only. The false alarms rate is plotted for each sensor and majority fuser as a function of threshold, which is chosen to from  $B/10$  to  $3B$  in steps of  $B/10$ , in Figure 3. The false alarm rate is 100% when threshold is at or below  $1.1B$ , and zero above that for all  $P_{0,1} = P_{1,0}$  values of 0.1, 0.01 and 0.001. The DTOA method correctly concluded no detection in this case with 298, 649, 965 measurements for  $P_{0,1} = P_{1,0}$  values of 0.1, 0.01 and 0.001, respectively.

The performance results for a source of strength  $A_S = 10^6$  is present are shown in Figure 4 and row 3 of Table I. This source results in an average radiation level of 1.17 times over the background level of  $B_{(x,y)} = 10$ . Based on the results above, to avoid high false alarm,

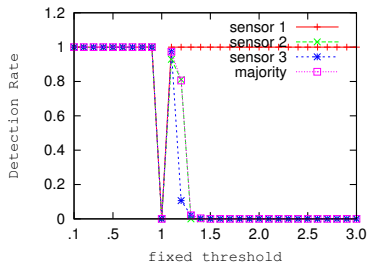


Figure 4: Detection rates for different thresholds for  $A_1 = 1.17B_{(x,y)}$ .

ave rad level at $M_1$	$M_1$ det (%)	majority det (%)	DTOA det (%)
$1.02 B_{(x,y)}$	1	0	65
$1.09 B_{(x,y)}$	16	10	100
$1.17 B_{(x,y)}$	51	96	100
$2.09 B_{(x,y)}$	99	100	100
$2.84 B_{(x,y)}$	99	100	100
$100.0 B_{(x,y)}$	100	100	100

Table 1: Summary of simulation results

the threshold  $\tau_H$  must be chosen above  $1.1B_{(x,y)}$ . For threshold  $\tau_H = 1.1B_{(x,y)}$ , the detection rates for  $M_1$ ,  $M_2$  and  $M_3$  are 0.99, 0.92 and 0.97, respectively; for threshold  $\tau_H = 1.2B_{(x,y)}$ , these rates are 0.81, 0 and 0.11. For thresholds  $\tau_H = 1.5B_{(x,y)}$  and higher only one sensor was able to detect the source. The DTOA method correctly concluded the detection in this case with 26, 100, 133 measurements for  $P_{0,1} = P_{1,0}$  values of 0.1, 0.01 and 0.001, respectively.

We now summarize the results based on batches of 100 randomly generated sources in Table I for different source strengths; average levels of radiation levels at the sensor  $M_1$  are shown in the first column of Table I. We show the detection rates of  $M_1$ , majority fuser for threshold  $\tau_H = 1.1B_{(x,y)}$ , and DTOA method in columns 2, 3 and 4 of Table I, respectively, for  $P_{0,1} = P_{1,0} = 0.01$ . The threshold is about 10% higher than the average background level, which is the suggested threshold level for radiation detection in practical scenarios [11]. While this threshold achieved zero false alarm rate, its detection rate depends on the source strength: it achieved close to 100% detection at  $M_1$  and majority fuser for higher source strengths that resulted in doubling of radiation levels at  $M_1$ . However for source strengths that lead to about 17% increase in the average radiation levels,  $M_1$  was only about 51% accurate although the majority fuser achieved 96% detection. DTOA method achieved 100% detection when average increase in radiation at  $M_1$  was at least 9% or higher above the background level.

## 4.2 Test-bed Results

Three radiation detection test-beds are set up at Oak Ridge National Laboratory, Purdue University, Uni-

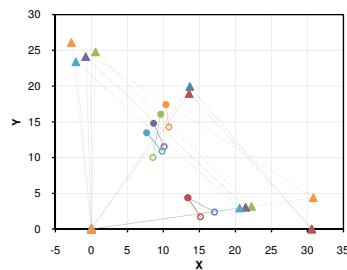


Figure 5: Localization results of a Cs-137 radiation source [15]. The triangle denotes sensors, filled circle denotes source location, and non-filled circle denotes estimated location. Different color denotes a different measurement set.

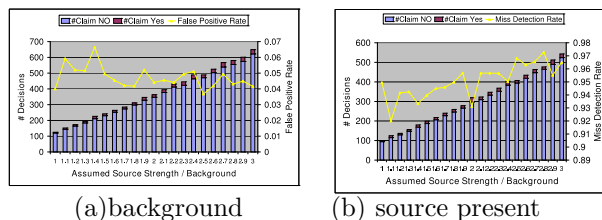


Figure 6: Testbed results for different thresholds.

versity of Illinois at Urbana-Champaign, all with the same configuration shown in Figure 2. A Cs-137 radiation source of strength  $0.95 \mu\text{-Curies}$  is used on a table top with RFTrax RAD-CZT sensors to collect measurements. Typically, detection and localization algorithms show almost identical performance on measurement sets collected on these testbeds.

For the testbed measurements we tested SPRT with  $\tau_H$  ranging from  $\hat{B}$  to  $3\hat{B}$ , where  $\hat{B}$  is the estimate of average background radiation level at  $M_1$ . In Figure 6(a), we show false alarm rate which is about 6% for  $\tau_H \leq 1.4\hat{B}$  and drops off to 4% for higher values. But when source is present, the detection rate is below 94% for  $\tau_H \leq 1.4\hat{B}$ , and 97% detection rate is achieved only for  $\tau_H \geq 2.7\hat{B}$ . DTOA achieved 100% detection with no false alarms on such measurement sets. In Figure 5(a), we show example cases with different source locations and their estimates using DTOA method [15]. When no source is present, the localization method returns ghost sources, as shown in the two examples in Figure 7, which were rejected by  $\mathcal{L}_{\hat{\delta}}$ .

## 5 Conclusions

We considered the detection problem of a source with scalar intensity inside a two-dimensional monitoring area using random sensor measurements in presence of a background process. We proposed a detection method that utilizes a robust localization method followed by an adaptive SPRT. Under Lipschitz smoothness and packing conditions on state-space, we showed that this method provides better performance com-

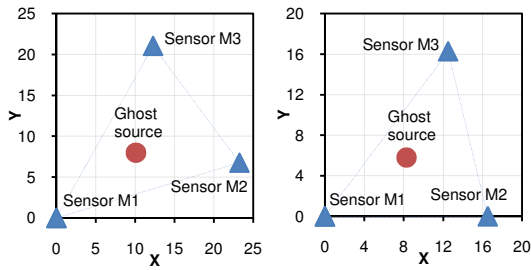


Figure 7: Ghost sources computed and rejected by DTOA [15].

pared to SPRT-based single sensor detectors, and also their majority and certain other fusers. Simulation and testbed results show the effectiveness of the proposed method for detecting point radiation sources.

There are several avenues for future work, including further simulation and test-bed experimentation. It would be of future interest to investigate the number of measurements needed by SPRT at sensors and fuser to reach a decision. It would be interesting to investigate SPRT detectors with multiple thresholds that can cover several spherical cells of the state-space. The idea of packing can be extended to different scales for different parameters and different thresholds at different sensors. It would also be interesting to pursue other methods that achieve superior performance compared to SPRT-based detection at the sensors.

## Acknowledgments

This work was funded by the SensorNet program at Oak Ridge National Laboratory which is managed by UT-Battelle, LLC for U.S. Department of Energy under Contract No. DE-AC05-00OR22725.

## References

- [1] D. E. Archer, B. R. Beauchamp, G. J. Mauger, K. E. Nelson, M. B. Mercer, D. C. Pletcher, V. J. Riot, J. L. Schek, and D. A. Knapp. Adaptable radiation monitoring system and method, 2006. U.S. Patent 7,064,336 B2.
- [2] S. M. Brennan, A. M. Mielke, and D. C. Torney. Radiation detection with distributed sensor networks. *IEEE Computer*, pages 57–59, August 2004.
- [3] J. C. Chin, C. Y. T. Ma, D. K. Y. Yau, N. S. V. Rao, M. Shankar, and Y. Yang. Accurate localization of low-level radioactive source under noise and measurement errors. In *The 6th ACM Conference on Embedded Networked Sensor Systems: Sensys*, 2008.
- [4] P. E. Felau. Comparing a recursive digital filter with the moving-average and sequential probability-ratio detection methods for SNM portal monitors. *IEEE Transactions on Nuclear Science*, 40(2):143–146, 1993.
- [5] A. Gunatilaka, B. Ristic, and R. Gailis. On localisation of a radiological point source. In *International Conference on Information, Decision and Control*. 2007.

- [6] K. D. Jarman, L. E. Smith, and D. K. Carlson. Sequential probability ratio test for long-term radiation monitoring. *IEEE Transactions on Nuclear Science*, 51(4):1662–1666, 2004.
- [7] N. L. Johnson. Sequential analysis: A survey. *Journal of Royal Statistical Society, Series A*, 124(3):372–411, 1961.
- [8] G. F. Knoll. *Radiation Detection and Measurement*. John Wiley, 2000.
- [9] A. Mielke, D. Jackson, S. M. Brennan, M. C. Smith, D. C. Torney, A. B. Maccabe, and J.F. Karlin. Radiation detection with distributed sensor networks. In *SPIE Defense and Security Proceedings*, 2005.
- [10] D. Mihalas and B. W. Mihalas. *Foundations of Radiation Hydrodynamics*. Courier Dover Publications, 2000.
- [11] K. E. Nelson, J. D. Valentine, and B. R. Beauchamp. Radiation detection method and system using the sequential probability ratio test, 2007. U.S. Patent 7,244,930 B2.
- [12] R. J. Nemzek, J. S. Dreicer, D. C. Torney, and T. T. Warnock. Distributed sensor networks for detection of mobile radioactive sources. *IEEE Transactions on Nuclear Science*, 51(4):1693–1700, 2004.
- [13] W. H. Press, S. A. Teukolsky, W. T. Vetterling, and B. P. Flannery. *Numerical Recipes in C*. Cambridge University Press, 1992.
- [14] N. S. V. Rao. Identification of simple product-form plumes using networks of sensors with random errors. In *International Conference on Information Fusion*, 2006.
- [15] N. S. V. Rao, M. Shankar, J. C. Chin, D. K. Y. Yau, S. Srivathsan, S. S. Iyengar, Y. Yang, and J. C. Hou. Identification of low-level point radiation sources using a sensor network. In *International Conference on Information Processing in Sensor Networks*, 2008.
- [16] N. S. V. Rao, M. Shankar, J. C. Chin, D. K. Y. Yau, Y. Yang, J. C. Hou, X. Xu, and S. Sahni. Localization under random measurements with application to radiation sources. In *International Conference on Information Fusion*, 2008.
- [17] N. S. V. Rao, X. Xu, and S. Sahni. A computational geometric method for dtoa triangulation. In *International Conference on Information Fusion*, 2007.
- [18] D. L. Stephens and A. J. Peurrung. Detection of moving radioactive sources using sensor networks. *IEEE Transactions on Nuclear Science*, 51(5):2273–2278, 2004.
- [19] A. Sundaresan, P. K. Varshney, and N. S. V. Rao. Distributed detection of a nuclear radioactive source using fusion of correlated decisions. In *International Conference on Information Fusion*, 2007.
- [20] H. L. Van Trees. *Detection, Estimation and Modulation Theory, Part I*. John Wiley, 1968.
- [21] P. K. Varshney. *Distributed Detection and Data Fusion*. Springer-Verlag, 1997.
- [22] G. B. Wetherill. *Sequential Methods in Statistics*. Methuen and Co., 1966.